Revista Brasileira de Física, Vol. 4, N.° 2, 1974

Multipole Analysis of Photoproduction of Pions from Protons*

J. R. RIOS LEITE and N. ZAGURY
Departamento de Física, *Pontifícia* Universidade Católica, Rio de Janeiro**

Recebido em 18 de maio de 1973

An energy dependent multipole analysis for photoproduction of π^+ and π^0 from threshold up to 450 MeV is presented.

Apresenta-se uma análise multipolar, dependente da energia, para a fotoprodução de π^+ e π^0, do limiar até 450 MeV.

Introduction

The purpose of this paper is to present a semi-phenomenological multipole analysis in pion photoproduction off protons at low energies.

Photoproduction of π^0 and π^+ around the first $\pi - n$ resonance are reasonably understood in terms of dispersion relation models which were first introduced by Chew, Goldberger, Low and Nambu'. Although the main experimental results can be explained by these models, there are severa1 uncertainties in the determination of the multipoles.

In the past few years, a number of phenomenological multipoles fits have been presented in the literature[2-6]. The most recent ones are those of Noelle, Pfeil and Schwela[5] and of Berends and Weaver[6]. Both fits are "energy-independent" and therefore they possess the advantage of not having a "biased" energy dependence in the multipoles. However, besides the problems of continuity in the solutions, there is the problem of non uniformity in the distribution of data through the whole range of angles and energies under consideration.

The purpose of this paper is to attempt an energy-dependent semi-phenomenological multipole analysis from threshold up to 450 MeV.

*Supported in part by B.N.D.E. and C.N.Pq.
**Postal address: Rua Marquês de S. Vicente, 209, 20000 — Rio de Janeiro GB.

In our approach, we take as first approximation a simple model and then ask for corrections in the multipoles with $J \leq 3/2$ that have an energy dependence which is the product of three factors:

(i) a phase as given by the Fermi-Watson theorem[7];

(ii) Threshold behaviour dependence;

(iii) A second degree polynomial in the energy.

The multipoles with high angular momentum ($J > 3/2$) will be fixed by the Born terms alone. As initial values for the multipoles, we will take the Born terms corrected for absorpiion except the resonant ones, which will be taken as $E_{1+}^{3/2} = 0$ and $M_{1+}^{3/2}$ equals to the C.G.L.N. value[1].

In Sec. 2, we give the necessary kinematics for the calculation; in Sec. 3, we present the model in some detail, while in Sec. 4, we exhibit the results; in Sec. 5, we summarize our conclusions.

2. General Results

In this section, we assemble several formulas that have been used in this analysis. Such formulas have been derived by several authors[8]. The most economical way to present them is to use the Jacob and Wick[8] helicity amplitudes. In photoprocluction, we can define 8 helicity amplitudes $H_{\lambda\mu}(\theta)$, where the labels refer to the final nucleon helicity λ_f and to the difference of the initial nucleon helicity λ_i and the photon helicity λ_γ. Parity conservation implies that

$$H_{\lambda\mu}(\theta) = -(-)^{\lambda-\mu} \, H_{-\lambda,-\mu}(\theta) \tag{2-1}$$

and therefore reduces the number of independent amplitudes to four. Following Ecklund and Walker[S], we call

$$H_1 = H_{1/2,3/2} = H_{-1/2,-3/2}, \quad H_3 = H_{-1/2,3/2} = -H_{1/2,-3/2},$$
$$H_2 = H_{1/2,1/2} = -H_{-1/2,-1/2}, \quad H_4 = H_{1/2,-1/2} = H_{-1/2,1/2}. \tag{2-2}$$

In this analysis, we will be concerned with four measurable quantities: the differential cross section, $\sigma(\theta)$, the polarized photon asymmetry, $\Sigma(\theta)$, the polarized target asymmetry, $T(\theta)$, and the polarization, $P(\theta)$, of the recoil nucleon (in a direction defined by k x q, where q and k are the pion and photon momenta, in the center of mass system respectively). The differential cross section and the polarization are given by

$$\sigma(\theta) = \frac{1}{2}\,\frac{q}{k}\sum_{i=1}^{4}\,|H_i|^2, \tag{2-3}$$

$$P(\theta) = -\frac{q}{k}\,\frac{1}{\sigma(\theta)}\ \mathrm{Im}\ (H_1 H_3^* + H_2 H_4^*)\cdot \tag{2-4}$$

The polarized photon asymmetry Σ is defined as the ratio between the difference and the sum of the cross sections by photons linearly polarized in a direction perpendicular ($\sigma_\perp$) and parallel ($\sigma_\parallel$) to the plane of reaction:

$$\Sigma(\theta) = \frac{\sigma_\perp - \sigma_\parallel}{\sigma_\perp + \sigma_\parallel} = \frac{q}{k}\,\frac{1}{\sigma(\theta)}\ \mathrm{Re}\ (H_1 H_4^* - H_2 H_3^*)\cdot \tag{2-5}$$

The polarized target asymmetry is defined as the ratio between the difference and sum of the cross sections on a proton target which is polarized parallel or antiparallel to the direction defined by q x k:

$$T(\theta) = \frac{q}{k}\,\frac{1}{\sigma(\theta)}\ \mathrm{Im}\ (H_1 H_2^* + H_3 H_4^*)\cdot \tag{2-6}$$

In the region of the first resonance, it is more convenient to work with the magnetic and electric multipoles instead of the partial wave helicity amplitudes. Therefore, we expand the H's directly in multipoles:

$$H_1 = \frac{1}{\sqrt{2}}\ \cos\frac{\theta}{2}\ \sin\theta \sum(E_{l+} - M_{l+} - E_{(l+1)-} - M_{(l+1)-})\,(P_l'' - P_{l+1}''), \tag{2-7}$$

$$H_2 = \frac{1}{\sqrt{2}}\ \cos\frac{\theta}{2} \sum[(l+2)E_{l+} + lM_{l+} + lE_{(l+1)-} - (l+2)M_{(l+1)-}]\,(P_l' - P_{l+1}'), \tag{2-8}$$

$$H_3 = \frac{1}{\sqrt{2}}\ \sin\frac{\theta}{2}\ \sin\theta \sum(E_{l+} - M_{l+} + E_{(l+1)-} + M_{(l+1)-})\,(P_l'' + P_{l+1}''), \tag{2-9}$$

$$H_4 = \frac{1}{\sqrt{2}}\ \sin\frac{\theta}{2} \sum[(l+2)E_{l+} + lM_{l+} - lE_{(l+1)-} + (l+2)M_{(l+1)-}]\,(P_l' + P_{l+1}'). \tag{2-10}$$

In order to use the Fermi-Watson theorem, we will write the two amplitudes $H^{\pi+}$ and H"", for π^+ and π^0 production, in terms of the amplitudes $H^{3/2}$ and $H^{1/2}$ for transitions to the $\mathbf{I} = 3/2$ and $\mathbf{I} = 1/2$ final isotopic spin states. Following the notation of Ref. 6, we have:

$$H^{\pi^+} = \sqrt{2}\left(H^{1/2} - \frac{1}{3} H^{3/2}\right),$$

$$H^{\pi^0} = H^{1/2} + \frac{2}{3} H^{3/2}. \qquad (2\text{-}11)$$

3. The Method

In this Section, we present a method for the deterrnination of the multipoles. We call $M^I_{l\pm}$ and E^I_{l+} the magnetic and electric multipoles leading to a final state with isotopic spin I, orbital angular momentum l and total angular momentum $\mathbf{j} = 1 \pm 1/2$. In what follows, we use the generic symbol $h^I_{l\pm}$ to denote either M^I_{l+} or E^I_{l+}. Thè method we have used is based in the following considerations:

i) The most important feature in ihis region of energies is the excitation of the first $\pi -$ n resonance;

ii) π^0 photoproduction can be understood in terms of low angular momenta only, but this is not true for π^+ production where a forward peak in the differential cross section is already present at energies as low as $k_{\mathrm{LAB}} \simeq 300$ MeV;

iii) By the Fermi-Watson[7] theorem, the phase, δ^I_{l+}, of the multipoles h^I_{l+}, are the same as the correspondirig $\pi -$ n scattering amplitudes below the threshold for production of two pions. As the inelasticity in $\pi -$ n scattering is, in this range, small, we extend the validity of the Fermi-Watson theorem to the whole region;

iv) Theoretical models using dispersion relation techniques have been presented in the literature[10]. It is found that the main features of the data can be explained reasonably well through the Born terms and a resonant magnetic amplitude.

Taking into account the above considerations, we assume that the multipoles are given by the sum of two terrns: $h^I_{l\pm}$ (INPUT) and $\Delta h^I_{l\pm}$. For all non-resonant amplitudes, $h^I_{l\pm}$(INPUT) is given by the Born contribution corrected for absorption:

$$h^I_{l\pm}(\mathrm{INPUT}) = (\text{Born contribution}).\ \exp\left(i\delta^I_{l\pm}\right) \cos \delta^I_{l+}, \qquad (3\text{-}1)$$

the resonant amplitudes $E_{1+}^{3/2}$(INPUT) is taken equal to zero and $M_{1+}^{3/2}$(INPUT) as the CGLN[1] value:

$$M_{1+}^{3/2} = \frac{\mu_p - \mu_n}{2} \frac{m_\pi}{f} \frac{k}{q^2} \exp(i\delta_{1+}^{3/2}) \sin \delta_{1+}^{3/2}, \quad (3\text{-}2)$$

where $f^2 \simeq 0.08$ and μ_p and μ_n are the total magnetic moments of proton and neutron.

The correction Δh_{l+}^I will be made only in the multipoles with $J \leq 3/2$: E_{0+}, M_{1-}, E_{1+}, M_{1+}, E_{2-}, M_{2-}. We assume that Δh is given by the product of three factors:

(i) $\exp(i\delta_{l\pm}^I)$ which assures the correct phase,
(ii) q^l which gives the correct threshold behaviour and
(iii) a second degree polynomial in the center-of-mass energy ω which will introduce an extra energy dependence:

$$a_{l\pm}^I + \omega\, b_{l\pm}^I + \omega^2\, c_{l+}^I, \quad (3\text{-}3)$$

a_{l+}^I, $b_{l\pm}^I$, $c_{l\pm}^I$ being a set of 36 parameters which are determined by comparison with the experimental data.

4. Results

The experimental results for the differential cross section, polarization of the recoil nucleon and photon asymmetry, were taken from Genzel and Pfeil[11]'s data collection. We also used the recent results of S. Arai et *al.*[12] for the polarized proton target asymmetry at 90^0. Table I shows the distribution of the data used among the several measurable quantities. The π – n phase shifts were taken from the Roper, Wright and Feld[13] analysis.

Table I — Distribution of the data analyzed in this paper.

	$\sigma(\theta)$	$P(\theta)$	$\Sigma(\theta)$	$T(\theta)$
π^+	869	5	97	7
π^0	670	24	30	0
Total	1539	29	127	7

The experimental results and the values of $h_{l\pm}$ (INPUT) were fed in a computer which was asked to find the 36 paranieters defined in the last chapter. The computer searched foi a mininium of the function:

$$\chi^2_\omega = \frac{1}{N} \sum_{i=1}^{N} \omega_i \left[\frac{Y^i_{\text{exp}} - Y^i_{\text{calc}}}{\Delta Y^i_{\text{exp}}} \right]^2, \tag{4-1}$$

where N is the number of events, $Y^i_{\text{exp}}, \Delta Y^i_{\text{exp}}, Y^i_{\text{calc}}$ are the experimental value, the total error and the calculated value for one of the measurable quantities, at a given angle and energy[14]; ω_i is a weight factor which will be defined below.

One of the problems that we have found in our analysis is the non uniformity in the distribution of the available data. Besides having only a few events in polarization and asymmetry experiments, the distribution of data in energy and angle for the differential cross section is quite nonuniform. In order to have an idea of the effect of this nonuniformity on the determination of the multipoles, we analyze the minimum of the χ^2_ω function in four separate casei:, A, B, *C* and D. In case A, we let $\omega_i \equiv 1$ as it is usually done. In cases B, C and D, all the experimental data were divided in sets $S^+_{\alpha\beta}$ ($S^0_{\alpha\beta}$) of events π^+ (π^0) having energy between E, and E, + ΔE, and cosθ between cosθ_β and cosθ_β + + Δ(cosθ), starting from E = 150 MeV and cosθ = − 1. In cases B, C and D, we put AE = 100 MeV, 60 MeV and 50 MeV and Δ(cosθ) = = 1/2, 1/3 and 1/4, respectively. Therefore, we have 24, 60 or 96 sets $S_{\alpha\beta}$. The weight ω_i was set equal to:

$$\omega_i = \frac{n}{n_i} \tag{4-2}$$

where n is the total number of events divided by the number of π^0 and π^+ sets, while n_i is the number of events in the set to which the given event "i" belongs. This weight would balance the importance between regions of unequal density of events. We note that $\omega_i = 1$ if the distribution of events is uniform among the sets.

	A	*B*	*C*	*D*
χ^2_ω	1.86	2.03	2.03	2.05

Table II — Values of the χ^2_ω — function for th: different solutions.

The results for the χ^2_ω functions are given in Table II. In each case, the parameters were obtained in two different ways. First, letting

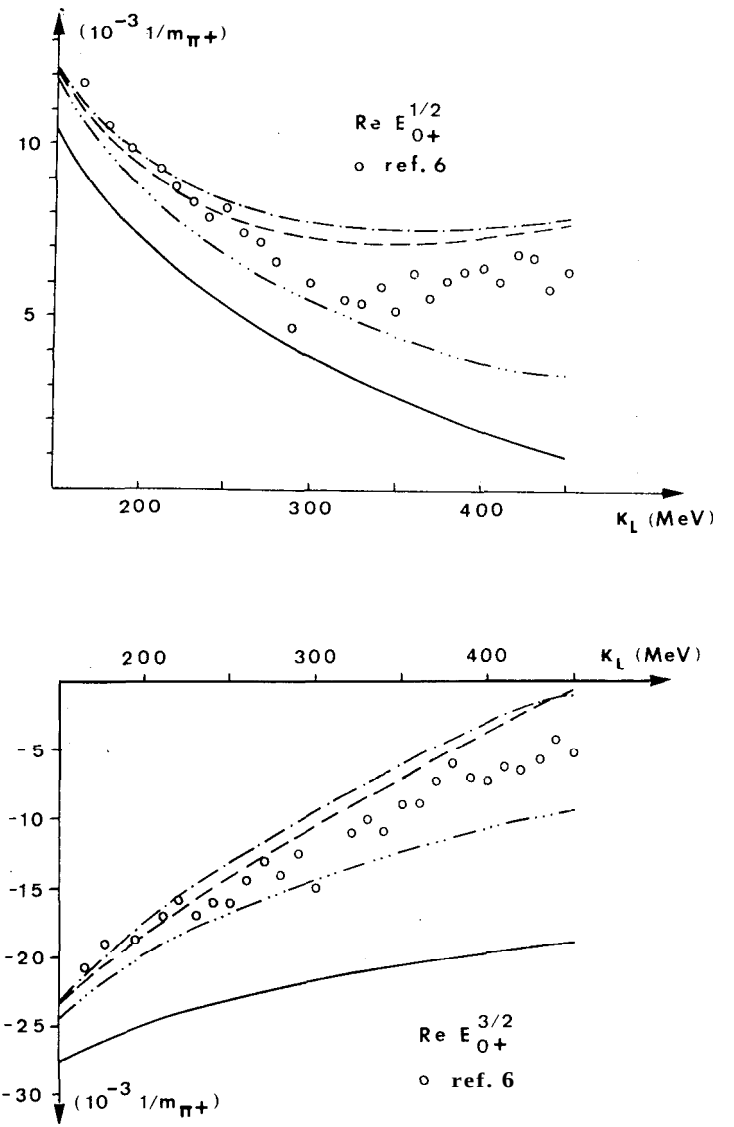

Fig. I — a) The real part of $E_{0+}^{1/2}$; b) The real part of $E_{0+}^{3/2}$. The solid line is the input. The dashed line, the — · — line and the — · · — line correspond to solutions A, B and D. The difference between solutions B and C are negligible and are not shown in the Figure.

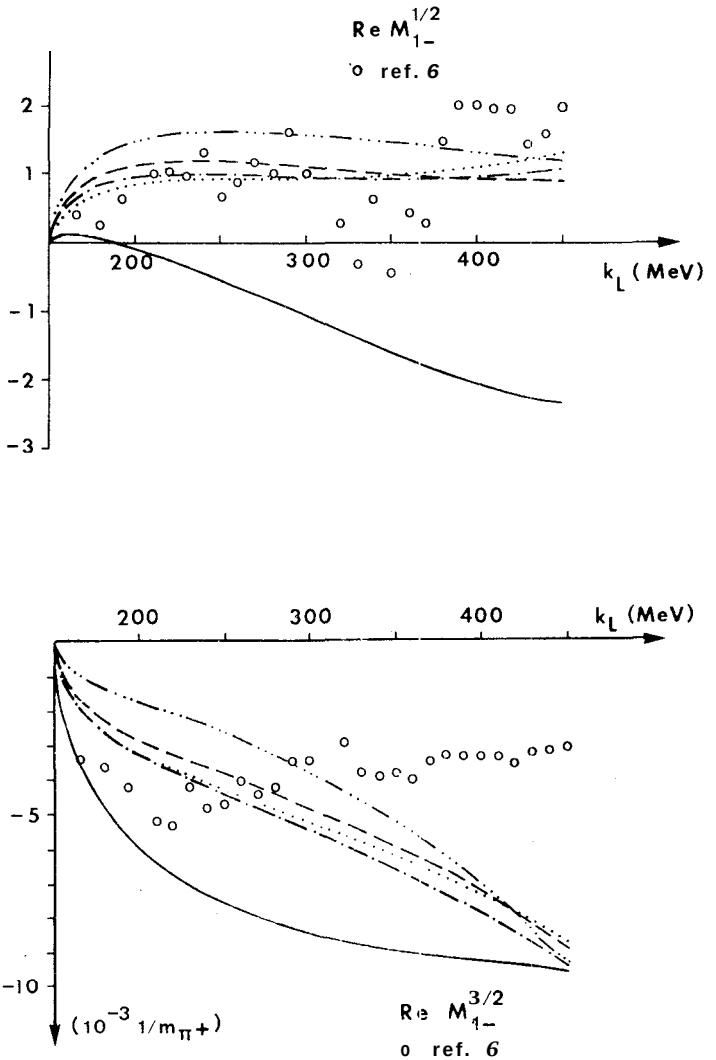

Fig. 2 — a) The real part of $M_1^{1/2}$; b) The real part of $M_1^{3/2}$. The solid line is the input. The dashed line, the $-\cdot-$ line, the dotted line and the $-\cdots-$ line correspond to solufions *A*, B, C and D.

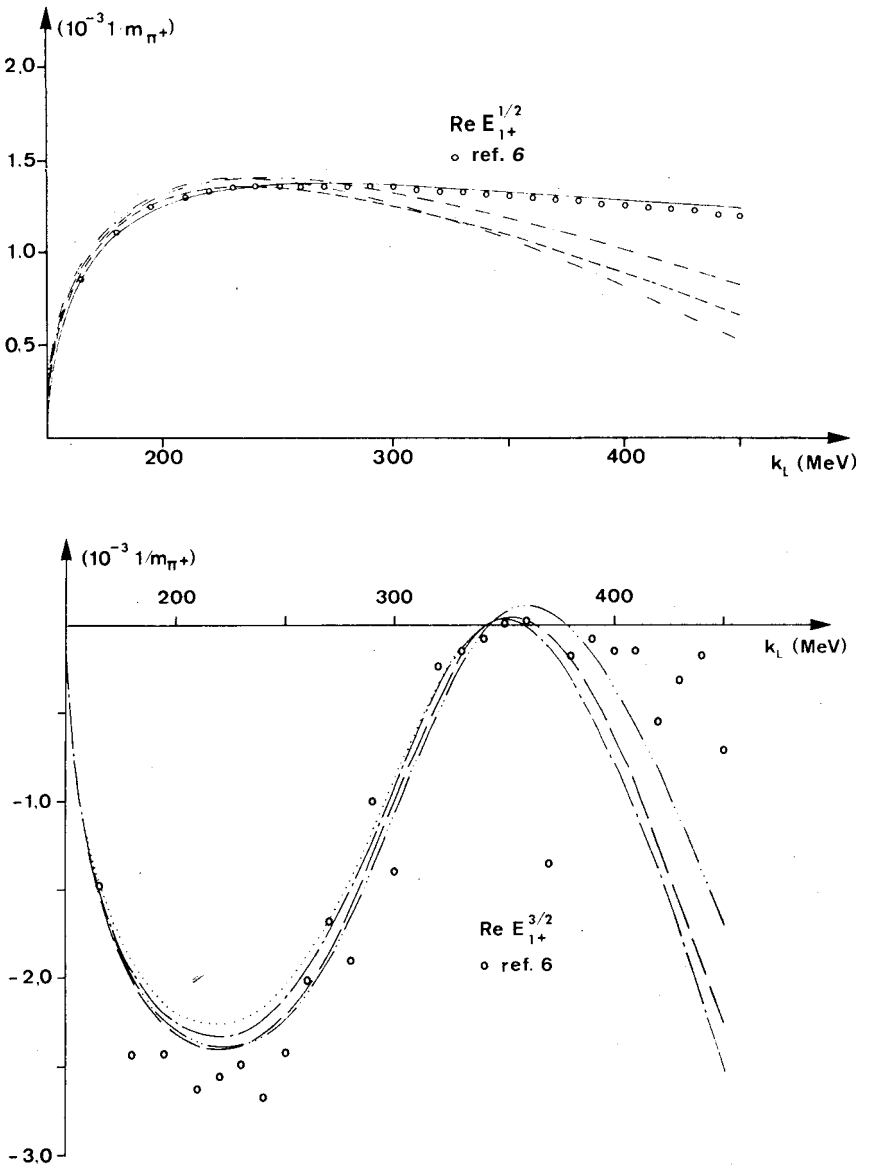

Fig. 3 — a) The real part of $E_{1+}^{1/2}$; b) The real part of $E_{1+}^{3/2}$. The solid line is the input. The dashed line, the $-\cdot-$ line, the dotted line and the $-\cdots-$ line correspond to solutions **A,** B, C and D. For $E_{1+}^{1/2}$ the difference between solutions B and C are negligible and are not shown in the Figure. For $E_{1+}^{3/2}$, the input is zero.

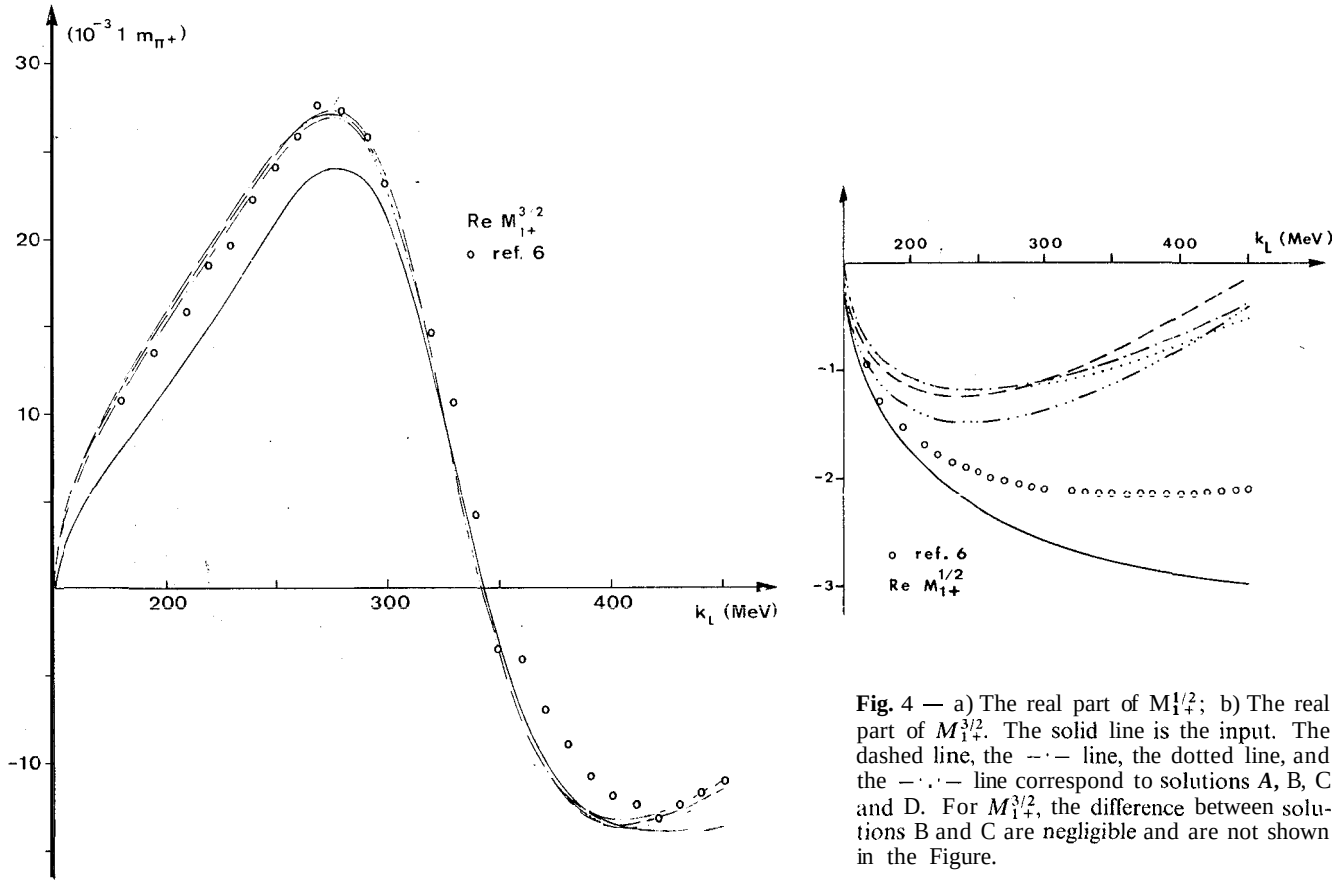

Fig. 4 — a) The real part of $M_{1+}^{1/2}$; b) The real part of $M_{1+}^{3/2}$. The solid line is the input. The dashed line, the – · – line, the dotted line, and the – · · – line correspond to solutions *A*, B, C and D. For $M_{1+}^{3/2}$, the difference between solutions B and C are negligible and are not shown in the Figure.

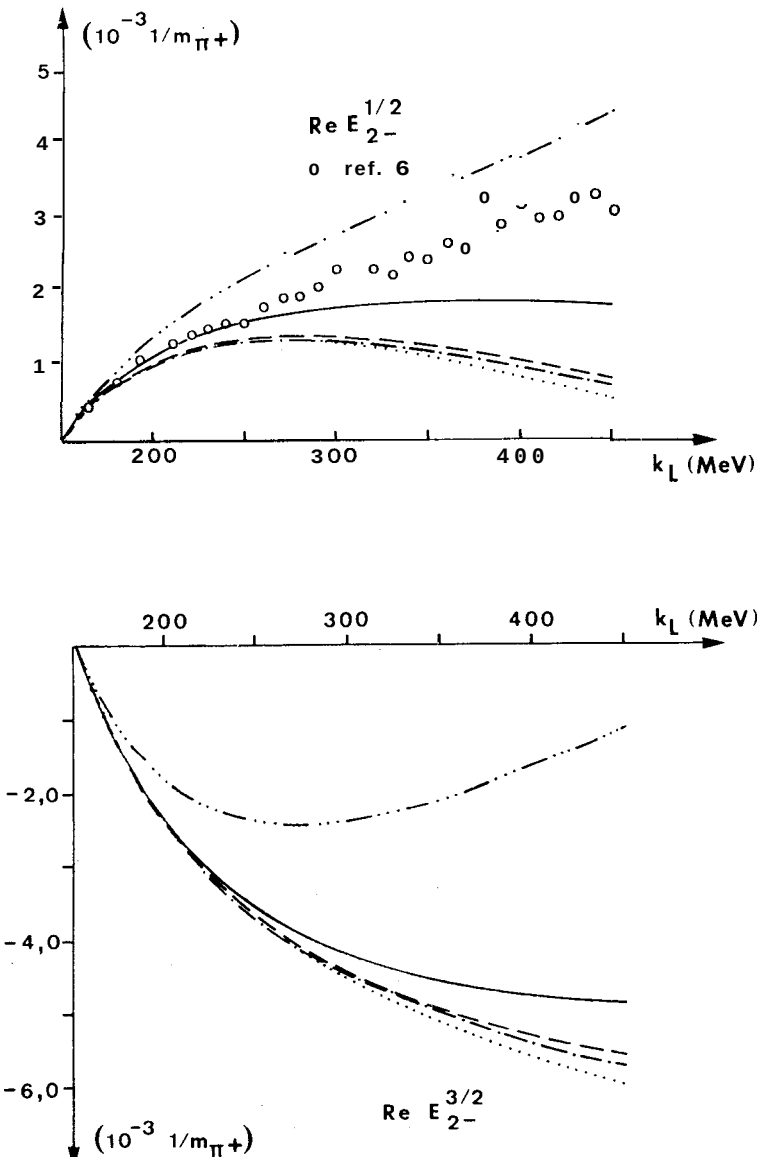

Fig. 5 — a) The real part of $E_{2-}^{1/2}$; b) The real part of $E_{2-}^{3/2}$. The solid line is the input. The dashed line, the $-.-$ line, the dotted line and the $-...-$ line correspond to solutions *A*, B, C and D.

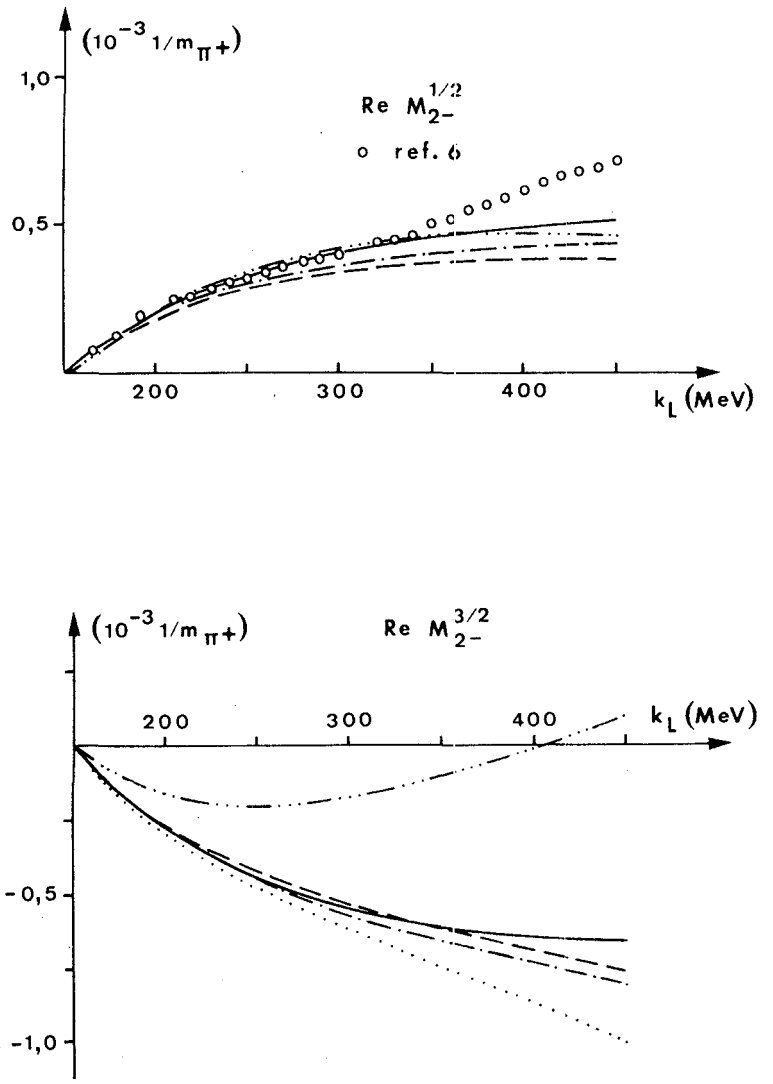

Fig. 6 — a) The real part of $M_{2-}^{1/2}$; b) The real par: of $M_{2-}^{3/2}$. The solid line is the input. The dashed line, the – · – line, the dotted line and the – · · · – lirie correspond to solutions A, B, C and D. For $M_{2-}^{1/2}$ the difference between solutions B and C are negligible and are not shown in the Figure.

only the E_{0+}, M_{1-}, M_{1+}, E_{1+} multipoles vary and then allowing variations on M_{2-} and E_{2-} and, second, letting all 36 parameters vary at once. The results are pratically the same, in both cases. Also, we have been able to check the effect of E_{2-} and M_{2-} multipoles in the variation of E_{0+}, M_{1-}, M_{1+} and E_{1+}. We have found that no appreciable effect exists.

Figs. 1 to 6 show the multipole solutions for cases ***A***, B, C and D. The graphs show that the multipoles M_{1+}, E_{1+}, $M_{2-}^{1/2}$, are quite stable as we move from one solution to another, this giving greater confidence in their determination. Also, solutions ***A***, B and C are quite close for all multipoles, but this is not true for solution D. This may be due to the fact that in this case there are sets $S_{\alpha\beta}$ that have as few events as 2, which is not statistically satisfactory. In Tables III and IV, we give numerical results for the multipoles in cases ***A*** and D.

In Figs. 1 to 6, we also show the values obtained by Berends and Weaver[6], for comparison. For a discussion of other multipole analyses, we refer to the work of Noelle et *al.*[5]. For the important multipole $M_{1+}^{3/2}$, our results are practically the same as those of Ref. 6. Also, they are very near to the CGLN value. For the large multipoles $E_{0+}^{1/2}$ and $E_{0+}^{3/2}$ and for $E_{2-}^{1/2}$, $E_{1+}^{3/2}$, their results lie, in general, in between our solutions ***A*** and D. For $M_{1+}^{1/2}$, their results are larger than ours, while for $E_{1+}^{1/2}$ and $M_{2-}^{1/2}$, they agree up to energies of $\sim$ 300 MeV. The most important differences occurs in the M_{1-} multipoles, mainly in the T = 3/2 channel. In fact, there are some difficulties in the determination of this multipole. It seems that the source of these difficulties is that the M_{1-} multipole appears in the differential cross section and in the photon asymmetry through linear combinations involving the large multipoles. Polarization experiments or polarized target experiments, however, should help in its determination. In fact, around the region of the first resonance, the only important terms will be those corresponding to the interference with $M_{1+}^{3/2}$ and $E_{1+}^{3/2}$. Disregarding multipoles with $l = 2$, we can write

$$\sigma(\theta)\, P(\theta) \simeq -\frac{q}{k} \sin \mathrm{O}\ \mathrm{Im}\left[(M_{1+} + 3E_{1+})(\mathrm{E}_{0+} - 3M_{1-} \cos \mathrm{O})^*\right], \quad \text{(4-3)}$$

$$\sigma(\theta)\, T(\theta) \simeq 3\frac{q}{k} \sin\theta.\ \mathrm{Im}\left[(M_{1+} - E_{1+})\ (E_{0+} - M_{1-}\ \cos\theta)\right]. \quad \text{(4-4)}$$

Unfortunately there are few experiments in nucleon recoil polarization or with polarized targets. Also it is important to have experiments

K_L	$E_{0+}^{1/2}$	$M_{1-}^{1/2}$	$E_{1+}^{1/2}$	$M_{1+}^{1/2}$	$E_{2-}^{1/2}$	$M_{2-}^{1/2}$	$E_{0+}^{3/2}$	$M_{1-}^{3/2}$	$E_{1+}^{3/2}$	$M_{1+}^{3/2}$	$E_{2-}^{3/2}$	$M_{2-}^{3/2}$
150	11.31	0.62	0.75	−0.65	0.29	0.04	−22.33	−1.38	−1.25	6.29	−0.65	−0.06
170	10.72	0.83	0.99	−0.87	0.53	0.08	−21.21	−1.89	−1.70	9.03	−1.21	−0.12
180	10.19	0.96	1.13	−1.00	0.72	0.12	−20.21	−2.25	−2.01	11.33	−1.69	−0.17
190	9.74	1.04	1.22	−1.10	0.87	0.15	−19.21	−2.57	−2.18	13.39	−2.10	−0.22
200	9.33	1.10	1.28	−1.17	1.00	0.18	−18.32	−2.83	−2.31	15.38	−2.46	−0.26
210	8.99	1.13	1.31	−1.21	1.10	0.21	−17.40	−3.07	−2.37	17.29	−2.78	−0.30
220	8.68	1.16	1.34	−1.24	1.18	0.23	−16.57	−3.27	−2.41	19.23	−3.06	−0.34
230	8.40	1.18	1.35	−1.25	1.24	0.25	−15.76	−3.47	−2.39	21.13	−3.31	−0.37
240	8.16	1.18	1.35	−1.25	1.29	0.27	−14.98	−3.67	−2.31	22.96	−3.54	−0.40
250	7.95	1.17	1.35	−1.24	1.32	0.29	−14.21	−3.86	−2.20	24.66	−3.74	−0.43
260	7.78	1.17	1.33	−1.23	1.35	0.30	−13.45	−4.05	−2.05	26.09	−3.92	−0.45
270	7.63	1.16	1.32	−1.21	1.36	0.32	−12.70	−4.25	−1.84	27.01	−4.08	−0.47
280	7.50	1.14	1.30	−1.18	1.37	0.33	−11.95	−4.45	−1.59	27.12	−4.23	−0.50
290	7.39	1.13	1.28	−1.14	1.37	0.34	−11.22	−4.65	−1.30	26.03	−4.37	−0.52
300	7.31	1.11	1.25	−1.10	1.36	0.35	−10.49	−4.86	−0.99	23.39	−4.49	−0.54
310	7.25	1.09	1.22	−1.05	1.35	0.36	−9.76	−5.09	−0.68	19.11	−4.61	−0.55
320	7.21	1.08	1.19	−1.90	1.33	0.36	−9.04	−5.30	−0.40	13.53	−4.72	−0.57
330	7.15	1.05	1.16	−0.95	1.31	0.37	−8.39	−5.51	−0.18	7.34	−4.82	−0.59
340	7.15	1.03	1.12	−0.90	1.28	0.37	−7.67	−5.76	−0.02	1.39	−4.91	−0.61
350	7.12	1.02	1.09	−0.84	1.26	0.38	−7.03	−5.98	0.04	−3.69	−4.99	−0.62
360	7.15	1.00	1.05	−0.78	1.22	0.38	−6.31	−6.24	0.03	−7.61	−5.08	−0.64
370	7.15	0.97	1.01	−0.72	1.19	0.38	−5.67	−6.49	−0.05	−10.39	−5.15	−0.65
380	7.20	0.96	0.97	−0.55	1.15	0.39	−4.97	−6.77	−0.21	−12.17	−5.22	−0.66
390	7.24	0.94	0.93	−0.59	1.12	0.39	−4.33	−7.03	−0.40	−13.20	−5.29	−0.68
400	7.31	0.94	0.88	−0.51	1.07	0.39	−3.63	−7.34	−0.65	−13.63	−5.36	−0.69
410	7.37	0.93	0.84	−0.45	1.03	0.39	−3.00	−7.62	−0.92	−13.67	−5.42	−0.71
420	7.43	0.92	0.80	−0.38	0.99	0.39	−2.37	−7.91	−1.22	−13.41	−5.48	−0.72
430	7.54	0.91	0.75	−0.30	0.95	0.39	−1.67	−8.25	−1.57	−12.90	−5.54	−0.73
440	7.63	0.91	0.70	−0.23	0.90	0.39	−1.04	−8.57	−1.92	−12.28	−5.59	−0.75
450	7.72	0.92	0.66	−0.15	0.86	0.38	−0.42	−8.89	−2.29	−11.56	−5.65	−0.76

Table III — Multipoles for solution *A*. K_L is given in MeV and multipoles in units of 10^{-3} x $\lambda_{\pi+}$.

K_L	$E_{0+}^{1/2}$	$M_{1-}^{1/2}$	$E_{1+}^{1/2}$	$M_{1+}^{1/2}$	$E_{2-}^{1/2}$	$M_{2-}^{1/2}$	$E_{0+}^{3/2}$	$M_{1-}^{3/2}$	$E_{1+}^{3/2}$	$M_{1+}^{3/2}$	$E_{2-}^{3/2}$	$M_{2-}^{3/2}$
160	11.00	0.79	0.77	−0.72	0.36	0.05	−23.44	−0.83	−1.22	6.12	−0.53	−0.05
170	10.33	1.07	1.01	−0.98	0.67	0.10	−22.42	−1.14	−1.66	8.79	−0.96	−0.08
180	9.72	1.25	1.16	−1.14	0.94	0.14	−21.53	−1.34	−1.97	11.04	−1.31	−0.11
190	9.18	1.36	1.25	−1.26	1.17	0.18	−20.67	−1.57	−2.14	13.07	−1.60	−0.14
200	8.68	1.45	1.31	−1.34	1.38	0.21	−19.92	−1.75	−2.28	15.03	−1.83	−0.16
210	8.23	1.51	1.35	−1.40	1.57	0.24	−19.18	−1.95	−2.34	16.94	−2.01	−0.18
220	7.82	1.56	1.37	−1.44	1.74	0.27	−18.52	−2.09	−2.39	18.87	−2.15	−0.19
230	7.43	1.60	1.39	−1.46	1.90	0.30	−17.90	−2.26	−2.38	20.77	−2.26	−0.19
240	7.08	1.61	1.39	−1.48	2.05	0.32	−17.31	−2.46	−2.32	22.60	−2.34	−0.20
250	6.75	1.62	1.38	−1.48	2.18	0.34	−16.75	−2.65	−2.22	24.31	−2.40	−0.20
260	6.45	1.63	1.37	−1.47	2.32	0.36	−16.22	−2.84	−2.08	25.77	−2.43	−0.20
270	6.17	1.62	1.35	−1.46	2.44	0.38	−15.71	−3.07	−1.89	26.71	−2.45	−0.19
280	5.90	1.61	1.32	−1.43	2.55	0.40	−15.23	−3.30	−1.65	26.86	−2.45	−0.19
290	5.66	1.60	1.29	−1.40	2.67	0.41	−14.76	−3.54	−1.38	25.81	−2.43	−0.18
300	5.42	1.59	1.26	−1.37	2.79	0.42	−14.32	−3.80	−1.07	23.23	−2.40	−0.17
310	5.21	1.56	1.23	−1.33	2.89	0.43	−13.89	−4.08	−0.76	19.00	−2.37	−0.16
320	5.00	1.55	1.19	−1.28	3.01	0.44	−13.47	−4.36	−0.46	13.45	−2.31	−0.15
330	4.81	1.52	1.15	−1.24	3.11	0.45	−13.10	−4.63	−0.22	7.31	−2.26	−0.13
340	4.63	1.50	1.11	−1.18	3.22	0.46	−12.72	−4.96	−0.03	1.38	−2.19	−0.12
350	4.45	1.47	1.07	−1.13	3.33	0.47	−12.37	−5.25	0.07	−3.68	−2.12	−0.10
360	4.29	1.45	1.02	−1.06	3.44	0.47	−12.01	−5.61	0.10	−7.60	−2.03	−0.08
370	4.14	1.41	0.97	−1.01	3.54	0.47	−11.69	−5.95	0.07	−10.39	−1.96	−0.07
380	3.99	1.39	0.92	−0.94	3.66	0.48	−11.36	−6.33	−0.03	−12.19	−1.86	−0.05
390	3.85	1.36	0.87	−0.88	3.76	0.48	−11.07	−6.70	−0.16	−13.25	−1.78	−0.03
400	3.73	1.34	0.82	−0.80	3.89	0.48	−10.76	−7.12	−0.36	−13.72	−1.67	−0.01
410	3.60	1.31	0.76	−0.73	4.00	0.48	−10.49	−7.52	−0.57	−13.80	−1.57	0.01
420	3.49	1.28	0.71	−0.66	4.11	0.48	−10.23	−7.93	−0.81	−13.60	−1.47	0.03
430	3.38	1.26	0.55	−0.58	4.23	0.48	−9.96	−8.41	−1.10	−13.15	−1.37	0.05
440	3.27	1.24	0.59	−0.50	4.35	0.47	−9.73	−8.86	−1.39	−12.59	−1.26	0.07
450	3.17	1.22	0.53	−0.43	4.47	0.47	−9.50	−9.32	−1.70	−11.93	−1.14	0.10

Table IV — Multipoles for solution *D*. K_L is given in MeV and multipoles in units of 10^{-3} x $\lambda_{\pi+}$.

both in the forward and backward directions in order to separate the M_{1-} term[15,16].

Figs. 7 to 12 show our results for the cross section for π^+ and π^0 production at three different energies. The curves show that solutions ***A,*** B, C, and D give pratically the same results except for π^0 production at forward and backward direction, where sol. D differs sligtly from the others.

In Figs 13 to 17, we show results for recoil nucleon polarization in π^0 production at 360 and 420 MeV and excitation curves for photon asymmetry and polarized target asymmetry. Here the differences between solutions *A,* B, C and solution D, appear more clearly.

5. Conclusions

From our analysis, we would like to make the following points:

i) Our values for χ^2_ω seems to confirm that the method of parametrization is a reasonable one;

ii) The values of E_{0+}, M_{1-}, M_{1+} and E_{1+} which we obtain are essentially independent of the adjustment of E_{2-} and M_{2-}. That is, the data are not stringent enough to determine E_{2-} and M_{2-} with confidence;

iii) Some multipoles are determined with more confidence than others. This is the case of $M_{1+}^{1/2}$, $M_{1+}^{3/2}$, $E_{1+}^{1/2}$, $E_{1+}^{3/2}$, $M_{2-}^{1/2}$;

iv) Our results, for the $M_1^{3/2}$ multipole, are quite different from other authors. Polarization and polarized target experiments should help in a better determination of this multipole;

v) The differences between solutions ***A,*** B and C and solution D may indicate that one needs more uniformity in the distribution of data, in order to have more confidence in the results of this type of analysis.

We would like to thank Mr. L. A. Diecher Sá and Mr. R. Gandelman for their help in some aspects of computer programming in the early part of this work.

References and Notes

1. G. F. Chew, M. L. Goldberger, F. E. Low and Y. Nambu, Phys. Rev. 106,1345 (1957).
2. M. Nigro and E. Schiavuta, Nuovo Cimento, 50, 358 (1967).
3. R. L. Walker, Phys. Rev. **182**, 1729 (1969).
4. Yu. M. Aleksandrov, V. F. Grushin and E. M. Leikin, Niicl. Phys. B 10, 145 (1969).
5. P. Noelle, W. Pfeil and D. Schwela, Nucl. Phys. B 26, 461 (1971).
6. F. A. Berends and D. L. Weaver, Nucl. Phys. B 30, 575 (1971).
7. K. Watson, Phys. Rev. 95, 228 (1954); E. Fermi, Suppl. Nuovo Cimento **2,** 58 (1955).
8. See, for example: W. Schmidt and G. Schwiderski, preprint, Kernforschungszentrum, Karlsruhe (1966); S. D. Ecklund and R. L. Walker, Phys. Rev. 159, 1195 (1967).
9. M. Jacob and C. Wick, Ann. Phys. **7,** 404 (1959).
10. See for example, S. Adler, Ann. Phys. 50, 189 (1968).
11. H. Genzel and W. Pfeil, Bonn Univ. PI B 1-168 (1972).
12. S. Arai *et al.*, Phys. Letters 40 B, 426 (1972).
13. L. D. Roper, R. M. Wright and B. T. Feld, Phys. Rev. **138** B, 190 (1965)
14. When only the statistical errors appear in the tables, a 5% systematic error was added to them.
15. A. Mullensiefen, Zeits. Phys. **188**, 199 (1965).
16. A. F. S. Penna and N. Zagury, An. Acad. Bras. Cienc. 42. 421 (1970).

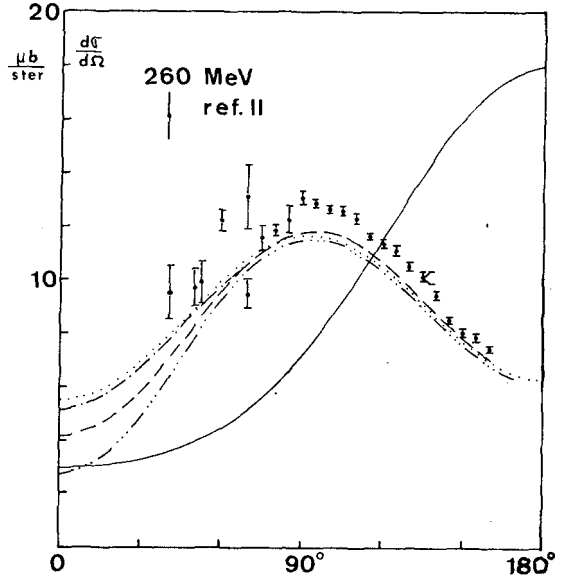

Fig. 7 — Cross section for π^0 photoproduction at 260 MeV. The solid line is the input. The dashed line, the —·— line, the dotted line and the —···— line correspond to solutions A, *B*, C and D.

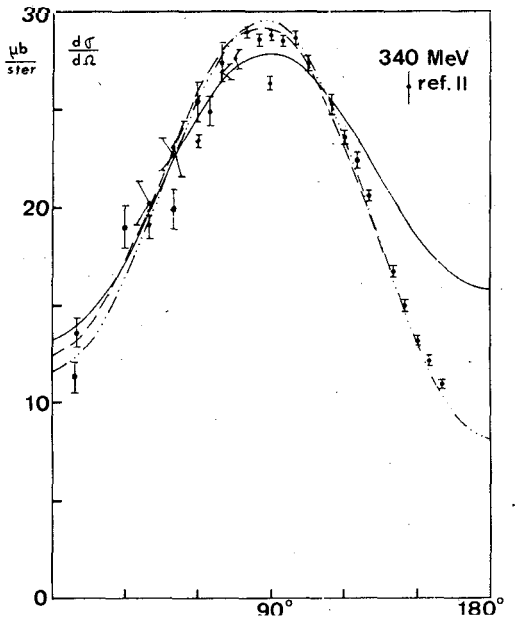

Fig. 8 — Cross section for π^0 photoproduction at *340* MeV. The solid line is the input. The dashed line and the —···— line correspond to solutions *A* and D. The differences between solutions *A*, B, C are small and are not shown.

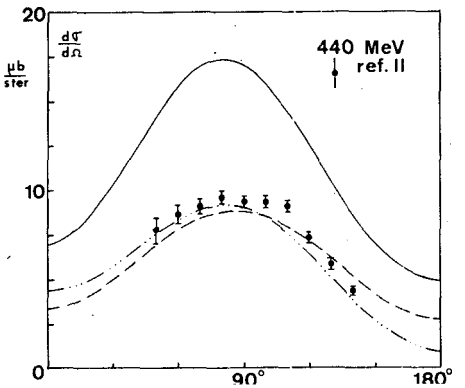

Fig. 9 — Cross section for π^0 photoprodtiction at *440* MeV. The solid line is the input. The dashed line and the —···— line correspond to solutions *A* and D. The differences between solutions *A*, B, C are small and are not shown.

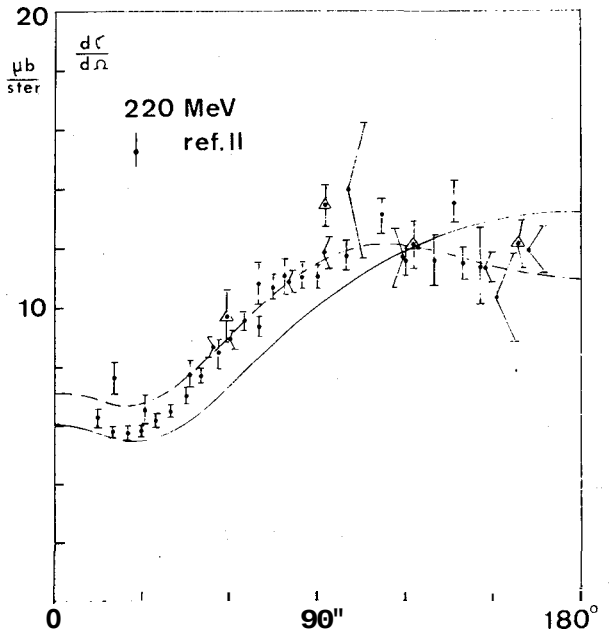

Fig. 10 - - Cross section for π^+ photoproduction at 220 MeV. The solid line is the inpiit and the dashed line is solution *A*. Tlic differences bctween solutions .4. R. C. *D* are small and are not shown.

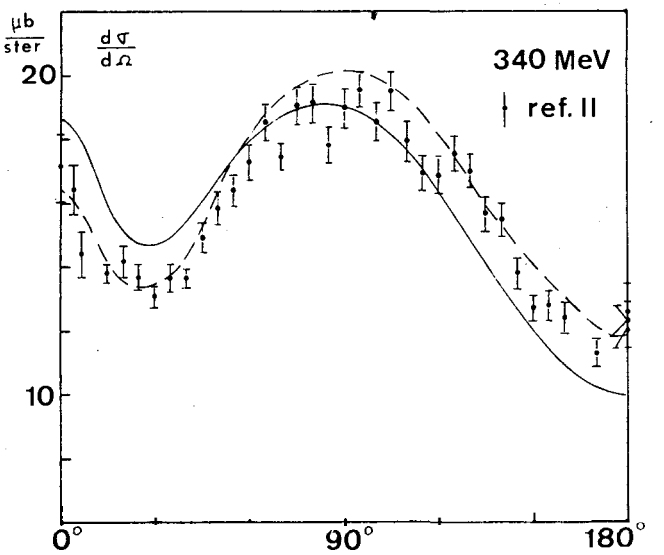

Fig. **11** — Cross section for π^+ photoproduction at 340 MeV. The solid line is the input and the dashed line is solution .A. Tlic differences between solutions **A**. B. C. *D* are small and are not shown.

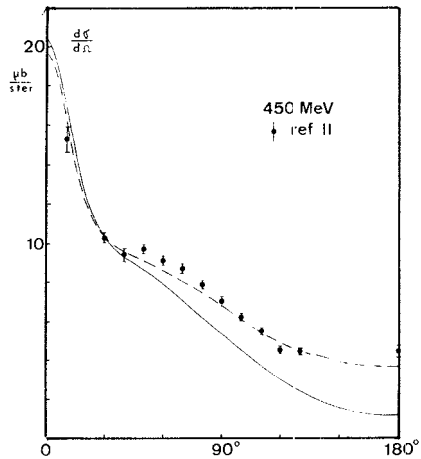

Fig. 12 — Cross section for π^+ photoproduction at 450 MeV. The solid line is the input and the dashed line is solution A. The differences betwecn solutions A, B, C, D are small and are not shown.

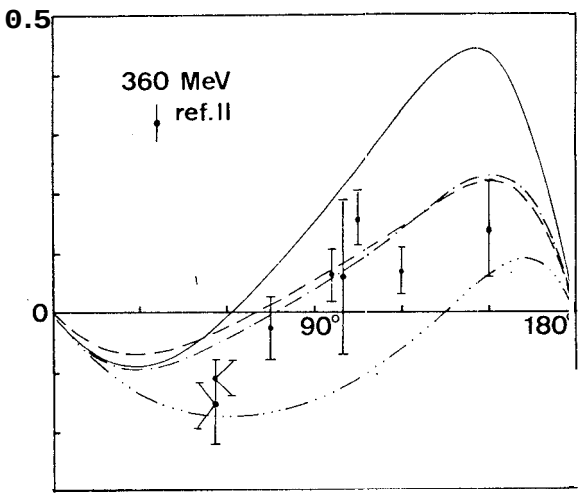

Fig. 13 — Nucleon recoil polarization in π^0 photoproduction at 360 MeV. The solid line is the input. The dashed line, thc – · – line, and the – · · · – line correspond to solutions A, B and D. The differenccs between solutions *A* and C are small and are not shown.

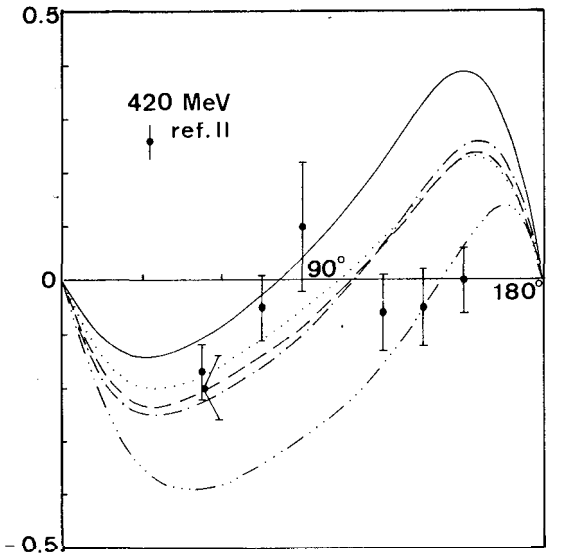

Fig. 14 — Nucleon recoil polarization in π^0 photoproduction at 420 MeV. The solid line is the input. The dashed line, the – · – line, the dotted line and the – · · · – line correspond to solutions *A*, B. C and *D*.

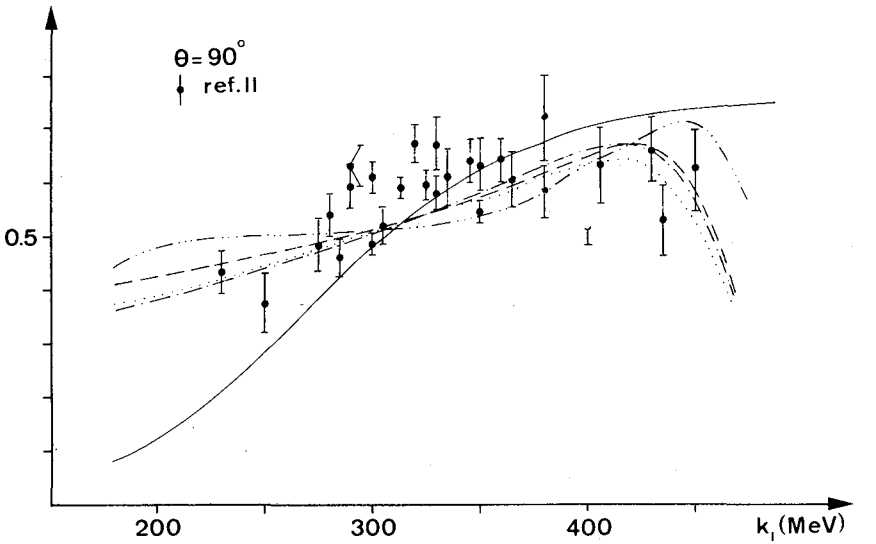

Fig. 15 Photon asymmetry excitation curve for π^0 photoproduction at 90 . The solid line is the input. The dashed line, tlie – · – linc. tlic dotted linc and the – · · · – line correspond to solutions A, B, C and B.

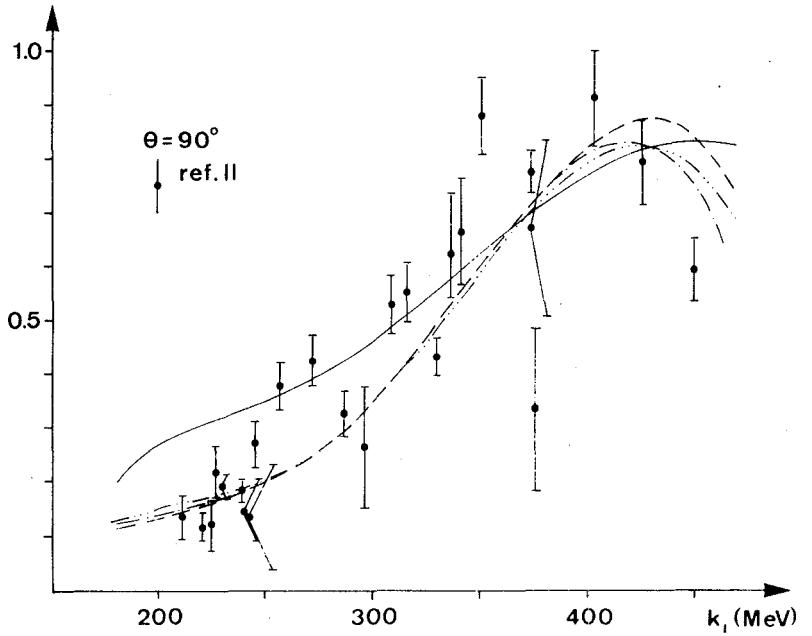

Fig. 16 — Photon asymmetry excitation curve for π^+ photoproduction at 90°. The solid line is the input. The dashed line, the – · – line and the – · · – line correspond to solutions **i.** H and *D*. The differences between solutions B and C are small and rire not shown.

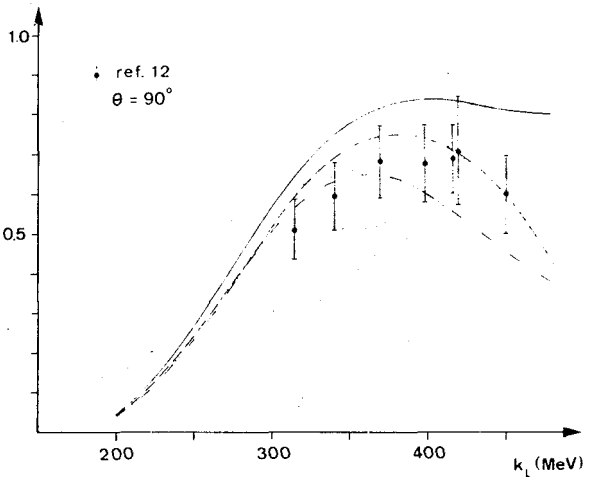

Fig. 17 — Polarized target asymmetry excitation curve for π photoproduction at 90". The solid line is the inpiit. The dashed line, the dotted line and the – · · – line correspond to solutions **A,** C and D. The differences between solutions A and B are small and are not shown.